Seasonal variation of secondary organic aerosol tracers in Central Tibetan Plateau

Ru-Qin Shen [a,c], Xiang Ding [a,*], Quan-Fu He [a,c], Zhi-Yuan Cong [b], Qing-Qing Yu [a,c], Xin-Ming Wang [a]

[a] State Key Laboratory of Organic Geochemistry, Guangzhou Institute of Geochemistry, Chinese Academy of Sciences, Guangzhou 510640, China

[b] Key Laboratory of Tibetan Environment Changes and Land Surface Processes, Institute of Tibetan Plateau Research, Chinese Academy of Sciences, Beijing 100085, China

[c] University of Chinese Academy of Sciences, Beijing, 100049, China

* Corresponding author

Dr. Xiang Ding

State Key Laboratory of Organic Geochemistry

Guangzhou Institute of Geochemistry, Chinese Academy of Sciences

511 Kehua Road, Guangzhou 510640, China

Tel: +86-20-85290127; Fax: +86-20-85290706

E-mail: xiangd@gig.ac.cn

Abstract

Secondary organic aerosol (SOA) affects the earth's radiation balance and global climate. High-elevation areas are sensitive to global climate change. However, at present, SOA origins and seasonal variations are understudied in remote high-elevation areas. In this study, particulate samples were collected from July 2012 to July 2013 at the remote Nam Co (NC) site, Central Tibetan Plateau and analyzed for SOA tracers from biogenic (isoprene, monoterpenes and β-caryophyllene) and anthropogenic (aromatics) precursors. Among these compounds, isoprene SOA (SOA_I) tracers represented the majority (26.6 ± 44.2 ng m^{-3}), followed by monoterpene SOA (SOA_M) tracers (0.97 ± 0.57 ng m^{-3}), aromatic SOA (SOA_A) tracer (2,3-dihydroxy-4-oxopentanoic acid, DHOPA, 0.25 ± 0.18 ng m^{-3}) and β-caryophyllene SOA tracer (β-caryophyllenic acid, 0.09 ± 0.10 ng m^{-3}). SOA_I tracers exhibited high concentrations in the summer and low levels in the winter. The similar temperature dependence of SOA_I tracers and isoprene emission suggested that the seasonal variation of SOA_I tracers at the NC site was mainly influenced by the isoprene emission. The ratio of high-NOx to low-NOx products of SOA_I (2-methylglyceric acid to 2-methyltetrols) was the highest in the winter and the lowest in the summer, due to the influence of temperature and relative humidity. The seasonal variation of SOA_M tracers was impacted by monoterpenes emission and gas-particle partitioning. During the summer to the fall, temperature effect on partitioning was the dominant process influencing SOA_M tracers' variation; while the temperature effect on emission was the dominant process influencing SOA_M tracers' variation during the winter to the spring. SOA_M tracer levels did not elevate with increased temperature in the summer, probably resulting from the counteraction of temperature effects on emission and partitioning. The concentrations of DHOPA were 1-2 orders of magnitude lower than those reported in the urban regions of the world. Due to the transport of air pollutants from the adjacent Bangladesh and the northeastern India, DHOPA presented relatively higher levels in the summer. In the winter when air masses mainly came from the northwestern India, mass fractions of DHOPA in total tracers increased, although its concentrations declined. The SOA-tracer method was applied to estimate secondary organic carbon (SOC) from these four precursors. The annual average of SOC was 0.22 ± 0.29 μgC m^{-3}, with the biogenic SOC (sum of isoprene, monoterpenes and β-caryophyllene) accounting for 75%. In the summer, isoprene was the major precursor with its SOC contributions of 81%. In the winter when the emission of biogenic precursors largely dropped, the contributions of aromatic SOC increased. Our study implies that anthropogenic pollutants emitted in

the Indian subcontinent could be transported to the TP and have impact on SOC over the remote NC.

Keywords: Secondary organic aerosol, Tibetan Plateau, Isoprene, Monoterpenes, Aromatics

1. Introduction

Organic aerosol affects the earth's radiation balance and global climate. As a large fraction of organic aerosol, secondary organic aerosol (SOA) is produced by homogenous (Claeys *et al.* 2004) and heterogeneous (Jang *et al.* 2002) reactions of volatile organic compounds (VOCs) as well as aging of organic aerosol (Robinson *et al.* 2007, Donahue *et al.* 2012). The global emission of biogenic VOCs (BVOCs), such as isoprene and monoterpenes (Guenther *et al.* 1995) were estimated to be one order of magnitude higher than those of anthropogenic sources (Piccot *et al.* 1992). Thus, global SOA is believed to be largely from BVOCs.

SOA tracers from specific VOCs can provide insight on processes and sources influencing SOA formation and spatiotemporal distribution. The identification of the isoprene SOA (SOA_I) tracers, 2-methyltetrols (Claeys *et al.* 2004) revealed the importance of SOA_I in global SOA burden. The further studies in high-NOx and low-NOx products of isoprene intermediates (e.g. methacrylic acid epoxide and isoprene epoxydiols) provided more details in the mechanisms of SOA_I formation under the influence of NOx (Paulot *et al.* 2009, Froyd *et al.* 2010, Surratt *et al.* 2010, Lin *et al.* 2013). The identification of tracers from aromatic SOA (SOA_A) (Offenberg *et al.* 2007) offered a way to directly evaluate the variation of anthropogenic SOA, particularly in urban regions. In addition, specific tracers have been determined in monoterpene SOA (SOA_M) (Jaoui *et al.* 2005, Claeys *et al.* 2007) and β-caryophyllene SOA (SOA_C) (Jaoui *et al.* 2007, van Eijck *et al.* 2013). Based on these SOA tracers, Kleindienst and coworkers further developed an SOA-tracer method to attribute SOA sources in the ambient air. Since it is difficult to directly measure SOA, the SOA-tracer method provides a valuable technique to estimate SOA in the ambient air, and it has been widely used around the world (Hu *et al.* 2008, von Schneidemesser *et al.* 2009, Guo *et al.* 2012, Lewandowski *et al.* 2013, Ding *et al.* 2014).

High-elevation areas are sensitive to global climate change (Xua *et al.* 2009). Observation of aerosol concentrations and compositions at high elevation sites can provide insight into the influence of natural and anthropogenic aerosols on global climate. The Tibetan Plateau (TP), the largest and highest plateau, is at the juncture of large desert areas and the densely populated Indian subcontinent. Previous

study found the northwesterly winds could bring dust from the western deserts to the TP and lead to high levels of geological aerosols at a site on the southeast TP (Zhao *et al.* 2013). Moreover, anthropogenic pollutants (e.g. sulfate, nitrate, potassium, element carbon, and heavy metals) emitted in the developing countries in South Asia could be transported to the TP by the southerly and southwesterly winds, especially during the summer monsoon season (Cong *et al.* 2007, Ming *et al.* 2010, Li *et al.* 2013, Zhao *et al.* 2013).

The observation at the remote central TP site, Nam Co (NC) discovered that the mean ratio of organic carbon (OC) to element carbon (EC) was 31.9 ± 31.1 during July 2006 to January 2007, implying the significant SOA contribution to OC (Ming *et al.* 2010) in the TP. However, there are only three studies in SOA compositions within the TP. Li et al. (2013) reported biogenic SOA (BSOA) tracers during the summer of 2010 at Qinghai Lake in the northeastern part of the TP. Stone et al., (2012) measured BSOA tracers from August to October 2005 on the south slope of Himalayas in the southwestern part of the TP. Due to the limited samples, it was difficult to examine the seasonal variation of these BSOA tracers in the TP. Moreover, due to the lack of anthropogenic SOA tracers, it was not possible to examine anthropogenic SOA in the TP, although above discussions have demonstrated that air pollutants from South Asia could be transported to the TP. Our recent study provided a snapshot of SOA tracers over China (including the NC and Linzhi sites in the TP) during the summer of 2012 (Ding *et al.* 2014). In this study, the observation at the remote NC site extended to one year. Seasonal trends of SOA tracers from isoprene, monoterpene, β-caryophyllene and aromatics were determined in the TP. Furthermore, secondary organic carbon (SOC) was estimated by the SOA-tracer method to check the variations of SOA origins at the NC site. To our knowledge, it is the first time that the seasonal trends of SOA tracers and origins are studied in the remote TP.

2. Experiment

2.1 Field Sampling

Samples were collected at a remote site (4730 meters above sea level) at the southeastern shore of Nam Co Lake in the central TP (Figure 1). Nam Co Lake (90°16′ – 91°03′ E and 30°30′ – 30°55′N) is located in the Nyainqen Tanglha Mountain Range with a total area of 2017 km^2 (Zhou *et al.* 2013). The major vegetation in the Nam Co Lake Basin is the high cold alpine meadow.

Sampling was undertaken from July 2012 to July 2013. An Anderson sampler equipped with

9-stage cascade impactors and pre-baked quartz fiber filters (Whatman, baked at 450 °C for 8 h) was used to get size-segregated particle samples at an air flow rate of 28.3 L min^{-1}. The 50% cutoff sizes are <0.4, 0.4−0.7, 0.7−1.1, 1.1−2.1, 2.1−3.3, 3.3−4.7, 4.7−5.8, 5.8−9.0, and ⩾9.0 μm, respectively. The flow rate was calibrated before and after each sampling episode using an airflow meter to ensure the sampler operated at the specified flow rate. One set of 9 size-fractionated filters were collected for 72 hours every two weeks. Additionally, four sets of field blanks were collected in the same way as the ambient samples for 5 minutes when the sampler was turned off. All samples were wrapped with aluminum foil and stored at -18°C before analysis.

2.2 Chemical Analysis

Each set of nine filters were combined together as one sample to meet the analysis requirement. Detailed information on the SOA tracer analysis is described elsewhere (Ding *et al.* 2014). Prior to solvent extraction, isotope-labeled standard mixtures were spiked into samples as internal standards. Samples were extracted twice by sonication with the mixed solvent dichloride methane (DCM)/hexane (1:1, v/v), then three times with the mixed solvent DCM/methanol (1:1, v/v). The extracts of each sample were combined, filtered and concentrated to ~2 mL. Then, the concentrated solution was divided into two parts for methylation and silylation, respectively.

The samples were analyzed by an a gas chromatography/mass spectrometer detector (GC/MSD, Agilent 7890/5975C) in the selected ion monitoring (SIM) mode with a 30 m HP-5 MS capillary column (i.d. 0.25 mm, 0.25 μm film thickness). Splitless injection of a 2 μL sample was performed. The GC temperature was initiated at 65 ºC, held for 2 min, then increased to 290 ºC at 5 ºC min^{-1} and held for 20 min. Thirteen SOA tracers were quantified by the GC/MSD coupled with an electron impact (EI) ionization source, including five SOA_M tracers (*cis*-pinonic acid, pinic acid, 3-methyl-1,2,3-butanetricarboxylic acid, 3-hydroxyglutaric acid and 3-hydroxy-4,4-dimethylglutaric acid), six SOA_I tracers (2-methylthreitol, 2-methylerythritol, 2-methylglyceric acid, *cis*-2-methyl-1,3,4-trihydroxy-1-butene, *trans*-2-methyl-1,3,4-trihydroxy-1-butene and 3-methyl-2,3,4-trihydroxy-1-butene), one SOA_C tracer (β-caryophyllenic acid) and one SOA_A tracer (2,3-dihydroxy-4-oxopentanoic acid, DHOPA). Figure S1 in supplemental information presents the total ion chromatogram (TIC) of these SOA tracers. *cis*-Pinonic acid and pinic acid were quantified by authentic standards. Due to the lack of standards, the SOA_I tracers were quantified using erythritol

(Claeys *et al.* 2004, Ding *et al.* 2008). The other SOA_M tracers were quantified using *cis*-pinonic acid. β-Caryophyllenic acid and DHOPA were quantified using octadecanoic acid and azelaic acid, respectively (Ding *et al.* 2012). The EI spectrum of each SOA tracer is shown in Figure S2-S4. The method detection limits (MDLs) for *cis*-pinonic acid, pinic acid, erythritol, octadecanoic acid and azelaic acid were 0.03, 0.05, 0.04, 0.03 and 0.07 ng m^{-3}, respectively, at a total volume of 122 m^3.

2.3 Quality assurance and quality control

Field and laboratory blanks were analyzed in the same manner as the field samples. These SOA tracers were not detected in the field or laboratory blanks. To evaluate the recoveries of the analytical method, six spiked samples (authentic standards spiked into solvent with pre-baked quartz filters) were analyzed. The recoveries were 101 ± 3 % for *cis*-pinonic acid, 70 ± 10 % for pinic acid, 65 ± 14 % for erythritol, 83 ± 7 % for octadecanoic acid, and 89 ± 9 % for azelaic acid. The relative differences for target compounds in samples collected in parallel (n=6) were all below 15%.

It should be noted that ketopinic acid was used as the surrogate for the quantification of all SOA tracers by Kleindienst et al. (2007); while different surrogates were used to quantify different SOA tracers in this study. The response factors of internal standard calibration for the 5 surrogates ranged from 0.98 (azelaic acid) to 1.78 (pinic acid), with the average of 1.38 and the relative standard deviation (RSD) of 23%. The response factor of ketopinic acid was also calculated in this study. Its value (1.27) was consistent with the average of the five surrogates.

2.4 Estimation of measurement uncertainty

Since there is no commercial standard available for most SOA tracers (except *cis*-pinonic acid and pinic acid), the use of surrogate standards for quantification introduces additional error to measurement. Error in analyte measurement (E_A) is propagated from the standard deviation of the field blank (E_{FB}), error in spike recovery (E_R) and the error from surrogate quantification (E_Q):

$$E_A = \sqrt{{E_{FB}}^2 + {E_R}^2 + {E_Q}^2} \quad (1)$$

Since SOA tracers were not detected in the field blanks, E_{FB} was 0 in this study. The spike recoveries of surrogate standards were used to estimate the E_R of tracers which ranged from 1% (*cis*-pinonic acid) to 35% (erythritol). Stone et al., (2012) developed an empirical approach to estimate E_Q based on homologous series of atmospherically relevant compounds. The relative error introduced

by each carbon atom (E_n) was estimated to be 15 %, each oxygenated functional group (E_f) to be 10% and alkenes (E_d) to be 60%. The errors introduced from surrogate quantification are treated as additive and are calculated as:

$$E_Q = E_n \Delta n + E_f \Delta \mathrm{f} + E_d \Delta \mathrm{d} \quad (2)$$

where Δn is the difference in carbon atom number between a surrogate and an analyte, Δf is the difference in oxygen-containing functional group between a surrogate and an analyte, Δd is the difference in alkene functionality between a surrogate and an analyte.

Table S1 shows the estimated uncertainties in tracer measurement. The errors from surrogate quantification (E_Q) ranged from 15% (2-methyltetrols) to 155% (β-caryophyllenic acid) in this study. Propagated with the error in recovery, the uncertainties in analyte measurement (E_A) were estimated in the range of 38% to 156%.

2.5 Backward trajectories

The air masses' transport during each sampling episode was investigated using Hybrid Single Particle Lagrangian Integrated Trajectory Model (HYSPLIT V4.9). Five-day backward trajectories (BTs) were analyzed during each sampling episode with 6-hour step at the height of 500 m above ground level. Then cluster analysis was performed to present the mean trajectory of each cluster, based on all the trajectories during our campaign.

3. Results and Discussions

3.1 Seasonal variations of SOA tracers

Since the NC site is located in the high elevation TP, the annual temperature was only -1.64 °C with the range of -16.1 °C in January to 10.2 °C in July (Table 1). The annual relative humidity (RH) was 58% with the peak in July (84%) and the lowest in January (30%). The sum of all tracers ranged from 0.78 to 185 ng m^{-3}. Among these compounds, SOA_I tracers (26.6 ± 44.2 ng m^{-3}) represented the majority, followed by SOA_M tracers (0.97 ± 0.57 ng m^{-3}), DHOPA (0.25 ± 0.18 ng m^{-3}) and β-caryophyllenic acid (0.09 ± 0.10 ng m^{-3}). During the summer (July-September 2012 and June-July 2013), SOA_I tracers presented the majority (> 95%). The mass fractions of SOA_M tracers in all compounds increased during the cold period (October 2012 to May 2013).

197

198 **3.1.1 Isoprene SOA tracers**

199 The total concentrations of SOA_I tracers (sum of six tracers) ranged from 0.36 – 184 ng m^{-3}. The
200 levels of SOA_I tracers were 1-2 orders of magnitude higher than those over the global oceans and the
201 Arctic (Table 2). Among the SOA_I traces, 2-methyltetrols (sum of 2-methylthreitol and
202 2-methylerythritol, MTLs) were the major components (72%), with an annual average of 23.8 ± 40.3
203 ng m^{-3} (0.18 to 165 ng m^{-3}). The 2-methylglyceric acid (MGA) averaged 1.95 ± 2.92 ng m^{-3} and
204 C_5-alkenetriols (sum of *cis*-2-methyl-1,3,4-trihydroxy-1-butene,
205 *trans*-2-methyl-1,3,4-trihydroxy-1-butene, and 3-methyl-2,3,4-trihydroxy-1-butene) averaged 0.93 ±
206 1.39 ng m^{-3}. MTLs are produced through the particle-phase uptake of the epoxydiols that formed in the
207 gas-phase photo-oxidation of isoprene under low-NOx or NOx free conditions (Paulot *et al.* 2009,
208 Surratt *et al.* 2010). Since the remote TP is a low-NOx environment, it is expected that the low-NOx
209 products, MTLs dominated over other SOA_I tracers. The majority of MTLs at the NC site was
210 consistent with those observed within the TP (Stone *et al.* 2012, Li *et al.* 2013) and over most global
211 oceans (Fu *et al.* 2011, Hu *et al.* 2013), but different from those over the North Pacific Ocean and the
212 Arctic where MGA was the major SOA_I tracer due to the significant influence of Siberian fires (Fu *et*
213 *al.* 2011, Ding *et al.* 2013). The two MTL isomers exhibited a strong correlation with each other
214 throughout the year (R^2=0.996, p<0.001) with a slope of 3.7, indicating that the two isomers shared
215 similar formation pathways.

216 Figure 2a presents a typical seasonal trend of SOA_I tracers that high concentrations all existed in
217 the summer. From October 2012 to April 2013, temperature was below zero, the levels of SOA_I tracers
218 dramatically decreased as low as 0.38 ng m^{-3} in January.

219 Isoprene emission rate (E_I) depends on light and temperature (Guenther *et al.* 1993):

220 $$E_I = EF_I \times C_L \times C_T \quad (3)$$

221 where EF_I is the basal emission rate at 30 °C leaf temperature and 1000 μmol m^{-2} s^{-1} PAR. C_L and C_T
222 are the factors representing the influences of light and temperature, respectively. C_T can be estimated
223 as:

224 $$C_T = \frac{exp^{\frac{C_{T1}(T-T_S)}{RT_STT}}}{1+exp^{\frac{C_{T2}(T-T_m)}{RT_STT}}} \quad (4)$$

225 Then the natural logarithm of C_T is calculated as:

$$\mathrm{Ln}\ C_T = \frac{C_{T1}}{RT_s}\left(1 - \frac{T_s}{T}\right) - \mathrm{Ln}[1 + exp^{\frac{C_{T2}}{RT_s}\left(1-\frac{T_m}{T}\right)}] \quad (5)$$

where R = 8.314 J K^{-1} mol^{-1}, C_{T1} = 95000 J mol^{-1}, C_{T2} = 230000 J mol^{-1}, T_s = 303 K, T_m = 314 K, and T is the leaf temperature (Guenther *et al.* 1993). Under the condition of $T < T_m$, the latter part in Equation (5) is close to zero, and Ln C_T is linearly correlated with 1/T.

Figure 3a presents a negative correlation between the natural logarithm of SOA_I tracer levels and the reciprocal of temperature in Kelvin ($p<0.001$). Moreover, the temperature dependence of SOA_I tracers was similar to that of C_T, and SOA_I tracers exhibited a significant positive correlation with C_T during our sampling at the NC site (Figure 3b). These results indicated that the seasonal variation of SOA_I tracers at the NC site was mainly influenced by the isoprene emission. Considering the short lifetime (several hours) of isoprene in the air, SOA_I should be mainly formed from local precursor. In summer, high temperature and intense light could enhance isoprene emission and photo-reactions. Moreover, high temperature in summer could enhance the heterogeneous reactions of isoprene-derived epoxides on particles which play the key roles in SOA_I formation (Lin et al., 2013; Paulot et al., 2009). All these interpreted the high levels of SOA_I tracers in the summer at the NC site. In the winter, isoprene emission significantly dropped due to the extremely low temperature. Thus, the tracers were only in trace amount at the NC site.

It is worth noting that the ratio of MGA to MTLs (MGA/MTLs) was negatively correlated with temperature (Figure 4a) and RH (Figure 4b). Based on chamber results, the formation mechanisms of MGA and MTLs are quite different. MGA is produced under high-NO_x conditions; while MTLs are mainly formed under low-NO_x or NO_x free conditions (Surratt *et al.* 2010). Moreover, low RH (15 – 40 %) could enhance the formation of MGA in the particulate phase but not of MTLs (Zhang *et al.* 2011). In addition, high particle acidity would favor the formation of MTLs instead of MGA (Surratt *et al.* 2007). Although there are few data available in the TP, the aerosols are expected to be neutral at the remote NC site. Thus, the influence of acidity on MGA/MTLs should be not significant. Isoprene emission is apparently high in summer due to high temperature and light intensity, which could enhance the ratio of isoprene to NOx and favor MTLs formation at the NC site. Moreover, high RH (~70%) in the summer (Table 1) could not favor MGA formation. Thus, MGA/MTLs exhibited the lowest values (less than 0.1) in the summer samples (Figure 4). In the winter, both temperature and RH dropped to the lowest of the whole year. Low temperature reduced isoprene emission and low RH

favored MGA formation. Thus, MGA/MTLs increased up to 0.8 in the winter samples (Figure 4).

3.1.2 Terpene SOA tracers

The total concentrations of SOA_M tracers (sum of five tracers) ranged from 0.11 – 2.39 ng m^{-3}. The levels of the SOA_M tracers were consistent with those over the global oceans and the Arctic (Table 2). Among these traces, *cis*-pinonic acid was the major compound (54%), with an annual average of 0.49 ± 0.38 ng m^{-3}, followed by pinic acid (0.22 ± 0.32 ng m^{-3}), 3-methyl-1,2,3-butanetricarboxylic acid (0.18 ± 0.25 ng m^{-3}), 3-hydroxyglutaric acid (0.08 ± 0.06 ng m^{-3}) and 3-hydroxy-4,4-dimethylglutaric acid (below MDL in the most samples).

The monthly variation of SOA_M tracers did not fully follow that of temperature (Figure 2b). From July to November 2012 (period 1), temperature decreased to -15 ºC; while SOA_M tracer levels increased as high as 1.99 ng m^{-3}. After that, both temperature and SOA_M tracers dropped to the lowest values in January 2013, and increased concurrently till April 2013 (period 2). During May to July 2013 (period 3), SOA_M tracer levels exhibited slight variation, although temperature kept increasing.

The seasonal variation of SOA_M tracers could be influenced by monoterpenes emission and gas-particle partitioning. Monoterpenes emission rate (E_M) is often assumed to be solely dependent on temperature (Guenther *et al.* 1993):

$$E_M = EF_M \times \gamma_T \quad (6)$$

$$\gamma_T = exp^{\beta(T-T_s)} \quad (7)$$

where EF_M is monoterpenes emission rate at a standard temperature T_s (303 K), γ_T is the activity factor by temperature, β is an empirical coefficient usually taken to be 0.09 K^{-1} (Guenther *et al.* 1993), T is the leaf temperature.

SOA yield (Y) of precursors could be expressed using an empirical relationship based on gas-particle partitioning of two semi-volatile products (Odum et al., 1996):

$$Y = M_0 \sum_i^2 \frac{\alpha_i K_i}{1+M_0 K_i} \quad (8)$$

where M_0 (μg m^{-3}) is the total concentration of absorbing organic material, α_i is the mass stoichiometric coefficients of the product i, K_i (m^3 μg^{-1}) is the temperature-dependent partitioning coefficient of the semi-volatile compound i. Assuming a constant activity coefficient and mean molecular weight, the partitioning coefficient, K_i (T) at a certain temperature (T) could be estimated as (Sheehan and

Bowman, 2001):

$$K_i(T) = K_i^* \frac{T}{T^*} \, exp\left[\frac{H_i}{R}\left(\frac{1}{T} - \frac{1}{T^*}\right)\right] \quad (9)$$

where K_i^* is an experimentally determined partitioning coefficient at a reference temperature, T^*. H_i is the vaporization enthalpy, R is the gas constant. To model the temperature-dependent absorptive partitioning, three parameters, α_i, K_i, and H_i, are required for each condensable product.

Table S2 lists all the parameters for two-product model of α-pinene SOA which were also used to estimate the temperature effect on SOA partitioning by Sheehan and Bowman (2001). The available data of OC at the NC site were reported in the range of 1.18 to 2.26 μgC m^{-3} during July 2006 to January 2007 with an average of 1.66 μgC m^{-3} (Ming et al., 2010). Thus, M_0 is calculated as 2.32 μg m^{-3} by the average OC multiplying 1.4. Figure S5 shows the temperature dependence of α-pinene emission rate (γ_T) and SOA yield within the temperature range at the NC site (-16.7 to 10.2 ºC). Obviously, decreasing temperature could reduce the emission but enhance the gas to particle partitioning and SOA yield.

From July to November 2012 (period 1), high values of SOA_M tracers and SOA yield existed under low temperature, and SOA_M tracers were positively correlated with SOA yield ($r=0.647$, $p<0.05$, Figure 5a). These suggested that the temperature effect on partitioning was the dominant process influencing SOA_M tracers' variation during the period 1. From December 2012 to April 2013 (period 2), high values of SOA_M tracers and activity factor (γ_T) existed under high temperature, and SOA_M tracers were positively correlated with γ_T ($r=0.741$, $p<0.05$, Figure 5b). These suggested that the temperature effect on emission was the dominant process influencing SOA_M tracers' variation during the period 2. The increase of SOA_M tracer concentrations during spring was also observed in the southeastern United States (Ding *et al.* 2008), resulting from the enhancement of monoterpenes emission in spring (Kim 2001). From May to July 2013 (period 3), SOA_M tracer concentrations were relative stable, and there was no correlation of SOA_M tracers with γ_T or SOA yield ($p>0.05$). These might result from the counteraction of temperature effects on emission and partitioning during the summer.

Previous study proposed that *cis*-pinonic acid and pinic acid (P) were the first-generation products of SOA_M and only formed under low-NOx conditions (Eddingsaas et al. 2012). The dominance of *cis*-pinonic acid and pinic acid among SOA_M tracers at the remote NC site indicated that SOA_M there was mainly formed under low-NOx conditions. Moreover, *cis*-pinonic acid and pinic acid could be

313 further photo-degraded to high-generation products, e.g. 3-methyl-1,2,3-butanetricarboxylic acid (M)
314 (Glasius et al. 2000; Jaoui et al. 2005; Szmigielski, et al., 2007). And the ratio of *cis*-pinonic acid plus
315 pinic acid to 3-methyl-1,2,3-butanetricarboxylic acid (P/M) could be applied to trace the aging of
316 SOA_M (Ding et al., 2011; Gómez-González et al., 2012). In the fresh chamber produced α-pinene SOA
317 samples, the ratios of P/M were reported in the range of 1.51 to 3.21 (Offenberg, et al., 2007). In this
318 study, the ratio of P/M averaged 16.7 ± 20.9. Thus, SOA_M was generally fresh at the NC site and
319 should be mainly formed from local precursors. Figure 6 presents a negative correlation between P/M
320 and temperature (r=-0.560, p=0.008). Higher P/M ratios were observed in the fall and the winter, and
321 lower P/M ratios occurred in the spring and the summer. Since temperature has positive influence on
322 photo-reaction rates, the higher temperature during the summer could accelerate the photochemistry in
323 the air and result in P to M conversion being more efficient. Thus, SOA_M in the summer was more aged
324 than that in the winter.

325 The levels of SOA_C tracer, β-caryophyllenic acid were in the range of below MDL to 0.40 ng m^{-3}.
326 As Figure 2c shows, the levels elevated from July to November 2012 and dropped to below MDL in
327 December 2012. Then, the concentrations increased from January to March 2013 and decreased from
328 April to June 2013. β-Caryophyllenic acid was positively correlated with SOA_M tracers (p=0.025),
329 indicating that the seasonal variation of β-caryophyllenic acid was similar with that of the SOA_M
330 tracers.

331

332 **3.1.3 Aromatic SOA tracer**

333 The levels of SOA_A tracer, DHOPA were in the range of below MDL to 0.61 ng m^{-3}. This
334 anthropogenic tracer was not detected or reported in global remote areas (Table 2). Due to few human
335 activity at the remote NC site, the highest concentration of DHOPA was 1-2 orders of magnitude lower
336 than those (up to 52 ng m^{-3}) reported in the urban regions of United States (Lewandowski *et al.* 2013)
337 and China (Ding *et al.* 2014). DHOPA exhibited the higher concentrations in the summer and the lower
338 levels in the winter (Figure 2d).

339 Besides urban emissions from solvent and fossil fuel use, biomass burning is an important source of
340 aromatics in many parts of the world (Lewis et al. 2013). The local dung or biomass burning (Duo et al.
341 2015; Xiao et al. 2015) may be potential sources of aromatics in the TP. Hence, DHOPA may come
342 from the processing of biomass burning emission. Figure 7 exhibits the monthly variation of biomass

burning tracer, levoglucosan during our sampling. The concentrations of levoglucosan ranged from 0.82 ng m^{-3} (October 2012) to 4.55 ng m^{-3} (April 2013) with a mean of 1.87±1.14 ng m^{-3}. Apparently, the monthly variation trend of levoglucosan was quite different from that of DHOPA. And there was no correlation between DHOPA and levoglucosan ($p>0.05$) (Figure S6). These indicated that DHOPA at the NC site was not mainly from the processing of biomass burning emission. Since there was few anthropogenic source near the remote NC site, the SOA_A tracer should be not locally formed but mainly transported from upwind regions.

To check the potential source areas of anthropogenic emissions, the satellite data of population density (http://sedac.ciesin.columbia.edu/theme/population), aerosol optical thickness (AOT, http://neo.sci.gsfc.nasa.gov/), tropospheric NO_2 vertical column densities (VCD, http://avdc.gsfc.nasa.gov/), and surface CO (https://www2.acd.ucar.edu/mopitt) were analysis on the global scale. As shown in Figure S7a, the northern Indian subcontinent was the most populated region of the world, with a population density of more than 1000 persons per km^2. Moreover, the plots of global AOT, tropospheric NO_2 VCD, and surface CO (Figure S7, b-d) all illustrated that the northern Indian subcontinent, including Bangladesh, Nepal, the northeastern India, and the northwestern India was the global hotspots of these anthropogenic pollutants. Compared with the northern Indian subcontinent, the TP exhibited extremely low population density and low levels of AOT, surface CO, and NO_2 VCD (Figure 8, a-d). Besides these satellite data, a recent study at a site in the northwestern India (Indo-Gangetic plain) witnessed extremely high levels (up to 2065 ng m^{-3}) of polycyclic aromatic hydrocarbons which were mainly formed from anthropogenic combustion processes (Dubey et al., 2015). All these demonstrated that there were high anthropogenic emissions in the northern India subcontinent.

The TP features a monsoon climate (Cong *et al.* 2007, Ming *et al.* 2010, Zhao *et al.* 2013). Figure 9a presents the average trajectory of each cluster during our sampling in the whole year. The air masses over the NC were primarily from Bangladesh, Nepal and the northeastern India (cluster 1, 32%), the northwestern India (Indo-Gangetic basin) (cluster 3–6, 55%), and the Taklimakan Desert (cluster 2, 13%) during the sampling period. In the summer, the prevailing southerly winds (cluster 1, Figure 9b) passed through the heavily polluted areas in the Bangladesh and the northeastern India, and could bring anthropogenic pollutants into the TP. Previous studies in the TP have witnessed the enrichment of anthropogenic metals (Cong *et al.* 2007) and the enhancement of carbonaceous aerosols (Ming *et al.*

2010, Zhao *et al.* 2013) under the influence of summer monsoon. Thus, the increase of DHOPA levels at the NC site in the summer was mainly due to the transport of air pollutants from the upwind Bangladesh and the northeastern India.

In the winter, the air masses over the NC site were mainly originated from the northwestern India (Indo-Gangetic basin) by the westerly winds (Figure 9b). Compared with the summer samples, the winter samples underwent the longer distance transport. Moreover, extremely low temperature in the winter could reduce DHOPA formation. Therefore, the levels of DHOPA were lower in the winter. It is worth noting that the mass fractions of DHOPA in all tracers significantly elevated in the winter (less than 2% in the summer but up to 10% in January, Figure 2d), although its levels reduced. As described in equation (3) and (6), temperature is an important factor controlling BVOCs emission. The drop of temperature from the summer (up to 10.2 ºC) to the winter (low to -16.7 ºC) at the NC site would lead to the emission of isoprene and monoterpenes decreasing by 98% and 90%, respectively. The elevated fractions of DHOPA in the winter samples suggested that the SOA contributions from aromatics would increase in the winter when BVOCs emission largely decreased.

3.2 Source apportionment

The SOA-tracer method developed by Kleindienst and co-workers was applied to attribute SOC at the NC site. The researchers performed chamber experiments to obtain the mass fraction of the tracers in SOC (f_{SOC}) for individual precursor:

$$f_{SOC} = \frac{\sum_i [tri]}{[SOC]} \quad (10)$$

where $\sum_i$[tri] is the total concentrations of the tracers for a certain precursor. [SOC] is the mass concentration of SOC. With these f_{SOC} values and the measured SOA tracers in the ambient air, SOC from different precursors can be estimated in the atmosphere, with the assumption that the f_{SOC} values in the chamber are the same as those in the ambient air. There is some degree of uncertainty in the SOA-tracer method due to the quantification with a single surrogate calibration standard (ketopinic acid) and the simplification of applying SOA tracers and conversion factors to calculate SOC in the ambient samples (Kleindienst *et al.* 2007). However, this method has been widely applied to attribute SOC from different precursors and proven to be able to provide reasonable results in the United States (Kleindienst *et al.* 2007, Stone *et al.* 2009, Lewandowski *et al.* 2013), and China (Hu *et al.* 2008, Guo

et al. 2012, Peng *et al.* 2013, Ding *et al.* 2014). Lewandowski et al. (2008) found that the measured OC in the midwestern United States could be fully explained by primary OC from chemical mass balance (CMB) model plus SOC from the SOA-tracer method, suggesting that the secondary organic tracer technique could be a valuable method for SOC estimation. Kleindienst et al. (2010) further compared the estimated SOC by the SOA-tracer method and other four independent methods (multiple regressions, CMB, carbon isotope and EC-tracer) in the southeastern United States, and found that these five methods matched well. Our previous study in the Pearl River Delta found SOC levels estimated by the SOA-tracer method were not only consistent with but also correlated well with those by EC-tracer method in summer, (Ding et al., 2012). The SOC apportionment results were also comparable between the SOA-tracer method and positive matrix factorization (PMF) model in Hong Kong (Hu et al. 2010).

The f_{SOC} were reported as 0.155 ± 0.039 μg μgC^{-1}, 0.023 ± 0.0046 μg μgC^{-1} and 0.00797 ± 0.0026 μg μgC^{-1} for isoprene (SOC_I), β-caryophyllene (SOC_C) and aromatics (SOC_A), respectively (Kleindienst *et al.* 2007). In this study, the same set of SOA tracers as reported by Kleindienst et al. (2007) were used for SOC estimation, including MGA and MTLs for SOC_I, β-caryophyllenic acid for SOC_C and DHOPA for SOC_A. For monoterpene SOC (SOC_M), nine tracers were involved in the source profile (Kleindienst *et al.* 2007). However, only five of the nine SOA_M tracers were measured in the current study. Wang et al. (2013) compared the results from model prediction with field observation in the Pearl River Delta and pointed out that the SOA-tracer method would underestimate SOA_M, probably due to the mismatch of tracer compositions in the field and the source profile (Ding *et al.* 2014). To minimize the uncertainty caused by the mismatch in tracer compositions, the f_{SOC} with the same five SOA_M tracers (0.059 μg μgC^{-1}) was computed using the chamber data from another study by the same research group (Offenberg *et al.* 2007). The same f_{SOC} for SOA_M was also applied to estimate SOC_M in our previous study over China (Ding *et al.* 2014).

The uncertainty in the SOA-tracer method is induced from the analysis of organic tracers and the determination of the conversion factors. Based on the E_A values in Table S1, the uncertainties in the tracer analyses were within 40% for SOA_I (only MGA and MTLs involved for SOC estimation), 95% for SOA_M, 156% for SOA_C, and 91% for SOA_A. The uncertainties of f_{SOC} were reported to be 25% for isoprene, 48% for monoterpenes, 22% for β-caryophyllene and 33% for aromatics (Kleindienst *et al.* 2007, Lewandowski *et al.* 2013). Considering these factors, the uncertainties of SOC apportionment

were calculated through error propagation. The RSD were 47% for SOC_I, 106% for SOC_M, 157% for SOC_C, and 96% for SOC_A. On average, the RSD of the reconstructed SOC (sum of the four precursors) was 51±11%.

Figure 10 presents the monthly variations of the reconstructed SOC. SOC was high in the summer 2012 and declined from October to December. After that, it kept increasing from January to June. The total concentrations of SOC ranged from 0.02 μgC m^{-3} to 0.69 μgC m^{-3} with an annual average of 0.22 ± 0.29 μgC m^{-3}. The available data of OC in total suspended particles at the NC site were reported in the range of 1.18 to 2.26 μgC m^{-3} during July 2006 to January 2007 (Ming *et al.* 2010). Since we did not measure OC in our size-segregated samples, the OC data reported by Ming et al. (2010) were used to calculate SOC fraction in OC (SOC/OC) from July to January. The calculated SOC/OC was average 38% in the summer and up to 58% in September, suggesting that SOC was an important contributor to OC at the NC site during the summer (Ming *et al.* 2010). However, from the fall to winter, the elevated OC and decreased SOC led to SOC/OC declining from 11% (in October) to 1% (in January), indicating that SOA from the four precursors had minor contributions to the elevated OC. Since the air masses during the fall to the winter were mostly originated from the northwestern Indo-Gangetic basin (cluster 3-6 in Figure 9), primary pollutants emitted there could transport to the TP and have significant impact on the air at the NC site. In addition, SOA from aqueous-phase reactions and primary OA aging could not be captured by the SOA-tracer method. Thus, the current results might underestimate the total amount of SOC, which partly explained the low OC shares of SOC at the NC site during the fall to the winter.

Biogenic SOC (sum of SOC_I, SOC_M, and SOC_C) dominated over SOC_A at the NC site, averagely accounting for 75% of the estimated SOC. In the summer, SOC_I was the major contributor with the SOC shares of 81%. From the fall to the spring, SOC_M became the major contributor, averagely contributing 38% to SOC. Although SOC_A levels reduced in the winter, SOC_A contributions elevated as high as 53% in January 2013. The elevated OC and the higher SOC_A contributions in the winter samples (Figure 10) implied that the transport of anthropogenic pollutants from the Indian subcontinent might have significant influence on carbonaceous aerosols over the remote NC during winter.

4. Conclusion

Seasonal trends of SOA tracers and origins were studied in the remote TP for the first time. SOA_I

tracers represented the majority among these compounds. The significant temperature dependence of SOA_I tracers suggested that the seasonal variation of SOA_I tracers at the NC site was mainly influenced by the isoprene emission. Due to the influence of temperature and relative humidity, the ratio of high-NOx to low-NOx products of SOA_I (MGA/MTLs) was the highest in the winter and the lowest in the summer. The seasonal variation of SOA_M tracers was impacted by monoterpenes emission and gas-particle partitioning. Due to the transport of air pollutants from the Indian subcontinent, DHOPA presented relatively higher concentrations in the summer and increased mass fractions in the winter. The SOA-tracer method was applied to estimated SOC from these four precursors. The annual average of SOC was 0.22 ± 0.29 μgC m^{-3}, with the biogenic SOC accounting for 75%. In the summer, isoprene was the major precursor with its SOC shares of 81%. In the winter when the emissions of biogenic precursors largely declined, the contributions of SOC_A increased. At present, SOA origins and their seasonal variations are unclear in the remote high-elevation TP. The remote TP is connected to the densely populated Indian subcontinent. Our study implies that anthropogenic pollutants emitted there could be transported to the TP and influence SOC over the remote NC.

Acknowledgment

This research was supported by the Strategic Priority Research Program of the Chinese Academy of Sciences (CAS) (XDA05100104/XDB05010200/XDA05100105), the National Science Foundation of China (41273116/41473099), and Youth Innovation Promotion Association, CAS.

References

Claeys, M., Graham, B., Vas, G., Wang, W., Vermeylen, R., Pashynska, V., Cafmeyer, J., Guyon, P., Andreae, M. O., Artaxo, P., and Maenhaut, W.: Formation of secondary organic aerosols through photooxidation of isoprene, Science, 303, 1173-1176, 2004.

Claeys, M., Szmigielski, R., Kourtchev, I., Van der Veken, P., Vermeylen, R., Maenhaut, W., Jaoui, M., Kleindienst, T. E., Lewandowski, M., Offenberg, J. H., and Edney, E. O.: Hydroxydicarboxylic acids: Markers for secondary organic aerosol from the photooxidation of alpha-pinene, Environ. Sci. Technol., 41, 1628-1634, 2007.

Cong, Z. Y., Kang, S. C., Liu, X. D., and Wang, G. F.: Elemental composition of aerosol in the Nam Co region, Tibetan Plateau, during summer monsoon season, Atmos. Environ., 41, 1180-1187, 2007.

Ding, X., Zheng, M., Yu, L. P., Zhang, X. L., Weber, R. J., Yan, B., Russell, A. G., Edgerton, E. S., and Wang, X. M.: Spatial and seasonal trends in biogenic secondary organic aerosol tracers and water-soluble organic carbon in the southeastern United States, Environ. Sci. Technol., 42, 5171-5176, 2008.

Ding, X., Wang, X., and Zheng, M.: The influence of temperature and aerosol acidity on biogenic secondary organic aerosol tracers: Observations at a rural site in the central Pearl River Delta region, South China, Atmos. Environ., 45, 1303-1311, 2011.

Ding, X., Wang, X. M., Gao, B., Fu, X. X., He, Q. F., Zhao, X. Y., Yu, J. Z., and Zheng, M.: Tracer-based estimation of secondary organic carbon in the Pearl River Delta, south China, J. Geophys. Res.-Atmos., 117, D05313, DOI: 10.1029/2011jd016596, 2012.

Ding, X., Wang, X. M., Xie, Z. Q., Zhang, Z., and Sun, L. G.: Impacts of Siberian biomass burning on organic aerosols over the North Pacific Ocean and the Arctic: Primary and secondary organic tracers, Environ. Sci. Technol., 47, 3149-3157, 2013.

Ding, X., He, Q.-F., Shen, R.-Q., Yu, Q.-Q., and Wang, X.-M.: Spatial distributions of secondary organic aerosols from isoprene, monoterpenes, β-caryophyllene, and aromatics over China during summer, J. Geophys. Res.-Atmos., 119, 11877-11891, 2014.

Donahue, N. M., Henry, K. M., Mentel, T. F., Kiendler-Scharr, A., Spindler, C., Bohn, B., Brauers, T., Dorn, H. P., Fuchs, H., Tillmann, R., Wahner, A., Saathoff, H., Naumann, K.-H., Moehler, O., Leisner, T., Mueller, L., Reinnig, M.-C., Hoffmann, T., Salo, K., Hallquist, M., Frosch, M., Bilde, M., Tritscher, T., Barmet, P., Praplan, A. P., DeCarlo, P. F., Dommen, J., Prevot, A. S. H., and Baltensperger, U.: Aging of biogenic secondary organic aerosol via gas-phase OH radical reactions, Proc. Natl. Acad. Sci. U. S. A., 109, 13503-13508, 2012.

Dubey, J., Maharaj Kumari, K., and Lakhani, A.: Chemical characteristics and mutagenic activity of PM2.5 at a site in the Indo-Gangetic plain, India, Ecotoxicol. Environ. Saf., 114, 75-83, 2015.

Duo, B., Zhang, Y., Kong, L., Fu, H., Hu, Y., Chen, J., Li, L., and Qiong, A.: Individual particle analysis of aerosols collected at Lhasa City in the Tibetan Plateau, J. Environ. Sci., 29, 165-177, 2015.

Eddingsaas, N. C., Loza, C. L., Yee, L. D., Chan, M., Schilling, K. A., Chhabra, P. S., Seinfeld, J. H., and Wennberg, P. O.: α-pinene photooxidation under controlled chemical conditions – Part 2: SOA yield and composition in low- and high-NOx environments, Atmos. Chem. Phys., 12, 7413-7427, 10.5194/acp-12-7413-2012, 2012.

Froyd, K. D., Murphy, S. M., Murphy, D. M., de Gouw, J. A., Eddingsaas, N. C., and Wennberg, P. O.: Contribution of isoprene-derived organosulfates to free tropospheric aerosol mass, Proc. Natl. Acad. Sci. U. S. A., 107, 21360-21365, 2010.

Fu, P. Q., Kawamura, K., Chen, J., and Barrie, L. A.: Isoprene, monoterpene, and sesquiterpene oxidation products in the high Arctic aerosols during late winter to early summer, Environ. Sci. Technol., 43, 4022-4028, 2009.

Fu, P. Q., Kawamura, K., and Miura, K.: Molecular characterization of marine organic aerosols collected during a round-the-world cruise, J. Geophys. Res.-Atmos., 116, D13302, DOI: 10.1029/2011jd015604, 2011.

Fu, P. Q., Kawamura, K., Chen, J., Charrière, B., and Sempéré, R.: Organic molecular composition of marine aerosols over the Arctic Ocean in summer: contributions of primary emission and secondary aerosol formation, Biogeosciences, 10, 653-667, 2013.

Glasius, M., Lahaniati, M., Calogirou, A., Di Bella, D., Jensen, N. R., Hjorth, J., Kotzias, D., and Larsen, B. R.: Carboxylic acids in secondary aerosols from oxidation of cyclic monoterpenes by ozone, Environ. Sci. Technol., 34, 1001-1010, 2000.

Gómez-González, Y., Wang, W., Vermeylen, R., Chi, X., Neirynck, J., Janssens, I. A., Maenhaut, W., and Claeys, M.: Chemical characterisation of atmospheric aerosols during a 2007 summer field campaign at Brasschaat, Belgium: sources and source processes of biogenic secondary organic aerosol, Atmos. Chem. Phys., 12, 125-138, 2012.

Guenther, A., Hewitt, C. N., Erickson, D., Fall, R., Geron, C., Graedel, T., Harley, P., Klinger, L., Lerdau, M., Mckay, W. A., Pierce, T., Scholes, B., Steinbrecher, R., Tallamraju, R., Taylor, J., and Zimmerman, P.: A global-model of natural volatile organic-compound emissions, J. Geophys. Res.-Atmos., 100, 8873-8892, 1995.

Guenther, A. B., Zimmerman, P. R., Harley, P. C., Monson, R. K., and Fall, R.: Isoprene and monoterpene emission rate variability - Model evaluations and sensitivity analyses, J. Geophys. Res.-Atmos., 98, 12609-12617, 1993.

Guo, S., Hu, M., Guo, Q., Zhang, X., Zheng, M., Zheng, J., Chang, C. C., Schauer, J. J., and Zhang, R.: Primary sources and secondary formation of organic aerosols in Beijing, China, Environ. Sci. Technol., 46, 9846-9853, 2012.

Hu, D., Bian, Q., Li, T. W. Y., Lau, A. K. H., and Yu, J. Z.: Contributions of isoprene, monoterpenes, β-caryophyllene, and toluene to secondary organic aerosols in Hong Kong during the summer of 2006, J. Geophys. Res.-Atmos., 113, D22206, DOI: 10.1029/2008jd010437, 2008.

Hu, D., Bian, Q., Lau, A. K. H., and Yu, J. Z.: Source apportioning of primary and secondary organic carbon in summer $PM_{2.5}$ in Hong Kong using positive matrix factorization of secondary and primary organic tracer data, J. Geophys. Res.-Atmos., 115, D16204, doi: 10.1029/2009JD012498, 2010.

Hu, Q. H., Xie, Z. Q., Wang, X. M., Kang, H., He, Q. F., and Zhang, P.: Secondary organic aerosols over oceans via oxidation of isoprene and monoterpenes from Arctic to Antarctic, Sci. Rep., 3, 2280, 2013.

Jang, M. S., Czoschke, N. M., Lee, S., and Kamens, R. M.: Heterogeneous atmospheric aerosol production by acid-catalyzed particle-phase reactions, Science, 298, 814-817, 2002.

Jaoui, M., Kleindienst, T. E., Lewandowski, M., Offenberg, J. H., and Edney, E. O.: Identification and quantification of aerosol polar oxygenated compounds bearing carboxylic or hydroxyl groups. 2.

565 Organic tracer compounds from monoterpenes, Environ. Sci. Technol., 39, 5661-5673, 2005.

566 Jaoui, M., Lewandowski, M., Kleindienst, T. E., Offenberg, J. H., and Edney, E. O.: β-Caryophyllinic
567 acid: An atmospheric tracer for β-caryophyllene secondary organic aerosol, Geophys. Res. Lett., 34,
568 L05816, DOI: 10.1029/2006gl028827, 2007.

569 Kim, J.-C.: Factors controlling natural VOC emissions in a southeastern US pine forest, Atmos.
570 Environ., 35, 3279-3292, 2001.

571 Kleindienst, T. E., Jaoui, M., Lewandowski, M., Offenberg, J. H., Lewis, C. W., Bhave, P. V., and
572 Edney, E. O.: Estimates of the contributions of biogenic and anthropogenic hydrocarbons to secondary
573 organic aerosol at a southeastern US location, Atmos. Environ., 41, 8288-8300, 2007.

574 Kleindienst, T. E., Lewandowski, M., Offenberg, J. H., Edney, E. O., Jaoui, M., Zheng, M., Ding, X.,
575 and Edgerton, E. S.: Contribution of primary and secondary sources to organic aerosol and PM2.5 at
576 SEARCH network sites, J. Air Waste Manage. Assoc., 60, 1388-1399, 2010.

577 Lewandowski, M., Jaoui, M., Offenberg, J. H., Kleindienst, T. E., Edney, E. O., Sheesley, R. J., and
578 Schauer, J. J.: Primary and secondary contributions to ambient $PM_{2.5}$ in the midwestern United States,
579 Environ. Sci. Technol., 42, 3303-3309, 2008.

580 Lewandowski, M., Piletic, I. R., Kleindienst, T. E., Offenberg, J. H., Beaver, M. R., Jaoui, M., Docherty,
581 K. S., and Edney, E. O.: Secondary organic aerosol characterisation at field sites across the United
582 States during the spring-summer period, Int. J. Environ. Anal. Chem., 93, 1084-1103, 2013.

583 Lewis, A. C., Evans, M. J., Hopkins, J. R., Punjabi, S., Read, K. A., Purvis, R. M., Andrews, S. J.,
584 Moller, S. J., Carpenter, L. J., Lee, J. D., Rickard, A. R., Palmer, P. I., and Parrington, M.: The
585 influence of biomass burning on the global distribution of selected non-methane organic compounds,
586 Atmos. Chem. Phys., 13, 851-867, 2013.

587 Li, J. J., Wang, G. H., Wang, X. M., Cao, J. J., Sun, T., Cheng, C. L., Meng, J. J., Hu, T. F., and Liu, S.
588 X.: Abundance, composition and source of atmospheric PM2.5 at a remote site in the Tibetan Plateau,
589 China, Tellus Ser. B-Chem. Phys. Meteorol., 65, 20281, DOI:10.3402/tellusb.v65i0.20281, 2013.

590 Lin, Y. H., Zhang, H. F., Pye, H. O. T., Zhang, Z. F., Marth, W. J., Park, S., Arashiro, M., Cui, T. Q.,
591 Budisulistiorini, H., Sexton, K. G., Vizuete, W., Xie, Y., Luecken, D. J., Piletic, I. R., Edney, E. O.,
592 Bartolotti, L. J., Gold, A., and Surratt, J. D.: Epoxide as a precursor to secondary organic aerosol
593 formation from isoprene photooxidation in the presence of nitrogen oxides, Proc. Natl. Acad. Sci. U. S.
594 A., 110, 6718-6723, 2013.

595 Ming, J., Xiao, C. D., Sun, J. Y., Kang, S. C., and Bonasoni, P.: Carbonaceous particles in the
596 atmosphere and precipitation of the Nam Co region, central Tibet, J. Environ. Sci., 22, 1748-1756,
597 2010.

598 Odum, J. R., Hoffmann, T., Bowman, F., Collins, D., Flagan, R. C., and Seinfeld, J. H.: Gas/particle
599 partitioning and secondary organic aerosol yields, Environ. Sci. Technol., 30, 2580-2585, 1996.

Offenberg, J. H., Lewis, C. W., Lewandowski, M., Jaoui, M., Kleindienst, T. E., and Edney, E. O.: Contributions of toluene and α-pinene to SOA formed in an irradiated toluene/α-pinene/NOx/ air mixture: Comparison of results using ^{14}C content and SOA organic tracer methods, Environ. Sci. Technol., 41, 3972-3976, 2007.

Paulot, F., Crounse, J. D., Kjaergaard, H. G., Kurten, A., St Clair, J. M., Seinfeld, J. H., and Wennberg, P. O.: Unexpected epoxide formation in the gas-phase photooxidation of isoprene, Science, 325, 730-733, 2009.

Peng, J. L., Li, M., Zhang, P., Gong, S. Y., Zhong, M. A., Wu, M. H., Zheng, M., Chen, C. H., Wang, H. L., and Lou, S. R.: Investigation of the sources and seasonal variations of secondary organic aerosols in PM2.5 in Shanghai with organic tracers, Atmos. Environ., 79, 614-622, 2013.

Piccot, S. D., Watson, J. J., and Jones, J. W.: A global inventory of volatile organic-compound emissions from anthropogenic sources, J. Geophys. Res.-Atmos., 97, 9897-9912, 1992.

Robinson, A. L., Donahue, N. M., Shrivastava, M. K., Weitkamp, E. A., Sage, A. M., Grieshop, A. P., Lane, T. E., Pierce, J. R., and Pandis, S. N.: Rethinking organic aerosols: Semivolatile emissions and photochemical aging, Science, 315, 1259-1262, 2007.

Sheehan, P. E., and Bowman, F. M.: Estimated effects of temperature on secondary organic aerosol concentrations, Environ. Sci. Technol., 35, 2129-2135, 2001.

Stone, E. A., Zhou, J., Snyder, D. C., Rutter, A. P., Mieritz, M., and Schauer, J. J.: A comparison of summertime secondary organic aerosol source contributions at contrasting urban locations, Environ. Sci. Technol., 43, 3448-3454, 2009.

Stone, E. A., Nguyen, T. T., Pradhan, B. B., and Dangol, P. M.: Assessment of biogenic secondary organic aerosol in the Himalayas, Environ. Chem., 9, 263-272, 2012.

Surratt, J. D., Lewandowski, M., Offenberg, J. H., Jaoui, M., Kleindienst, T. E., Edney, E. O., and Seinfeld, J. H.: Effect of acidity on secondary organic aerosol formation from isoprene, Environ. Sci. Technol., 41, 5363-5369, 2007.

Surratt, J. D., Chan, A. W. H., Eddingsaas, N. C., Chan, M. N., Loza, C. L., Kwan, A. J., Hersey, S. P., Flagan, R. C., Wennberg, P. O., and Seinfeld, J. H.: Reactive intermediates revealed in secondary organic aerosol formation from isoprene, Proc. Natl. Acad. Sci. U. S. A., 107, 6640-6645, 2010.

Szmigielski, R., Surratt, J. D., Gómez-González, Y., Veken, P. V. d., Kourtchev, I., Vermeylen, R., Blockhuys, F., Jaoui, M., Kleindienst, T. E., Lewandowski, M., Offenberg, J. H., Edney, E. O., Seinfeld, J. H., Maenhaut, W., and Claeys, M.: 3-Methyl-1,2,3-butanetricarboxylic acid: An atmospheric tracer for terpene secondary organic aerosol, Geophys. Res. Lett., 34, L24811, doi:10.1029/2007GL031338, 2007

van Eijck, A., Opatz, T., Taraborrelli, D., Sander, R., and Hoffmann, T.: New tracer compounds for secondary organic aerosol formation from beta-caryophyllene oxidation, Atmos. Environ., 80, 122-130, 2013.

636 von Schneidemesser, E., Schauer, J. J., Hagler, G. S. W., and Bergin, M. H.: Concentrations and
637 sources of carbonaceous aerosol in the atmosphere of Summit, Greenland, Atmos. Environ., 43,
638 4155-4162, 2009.

639 Wang, S. Y., Wu, D. W., Wang, X. M., Fung, J. C. H., and Yu, J. Z.: Relative contributions of secondary
640 organic aerosol formation from toluene, xylenes, isoprene, and monoterpenes in Hong Kong and
641 Guangzhou in the Pearl River Delta, China: an emission-based box modeling study, J. Geophys.
642 Res.-Atmos., 118, 507-519, 2013.

643 Xiao, Q., Saikawa, E., Yokelson, R. J., Chen, P., Li, C., and Kang, S.: Indoor air pollution from burning
644 yak dung as a household fuel in Tibet, Atmos. Environ., 102, 406-412, 2015.

645 Xua, B., Cao, J., Hansen, J., Yao, T., Joswia, D. R., Wang, N., Wu, G., Wang, M., Zhao, H., Yang, W.,
646 Liu, X., and He, J.: Black soot and the survival of Tibetan glaciers, Proc. Natl. Acad. Sci. U. S. A., 106,
647 22114-22118, 2009.

648 Zhang, H., Surratt, J. D., Lin, Y. H., Bapat, J., and Kamens, R. M.: Effect of relative humidity on SOA
649 formation from isoprene/NO photooxidation: enhancement of 2-methylglyceric acid and its
650 corresponding oligoesters under dry conditions, Atmos. Chem. Phys., 11, 6411-6424, 2011.

651 Zhao, Z. Z., Cao, J. J., Shen, Z. X., Xu, B. Q., Zhu, C. S., Chen, L. W. A., Su, X. L., Liu, S. X., Han, Y.
652 M., Wang, G. H., and Ho, K. F.: Aerosol particles at a high-altitude site on the Southeast Tibetan
653 Plateau, China: Implications for pollution transport from South Asia, J. Geophys. Res.-Atmos., 118,
654 11360-11375, 2013.

655 Zhou, S. Q., Kang, S. C., Chen, F., and Joswiak, D. R.: Water balance observations reveal significant
656 subsurface water seepage from Lake Nam Co, south-central Tibetan Plateau, J. Hydrol., 491, 89-99,
657 2013.

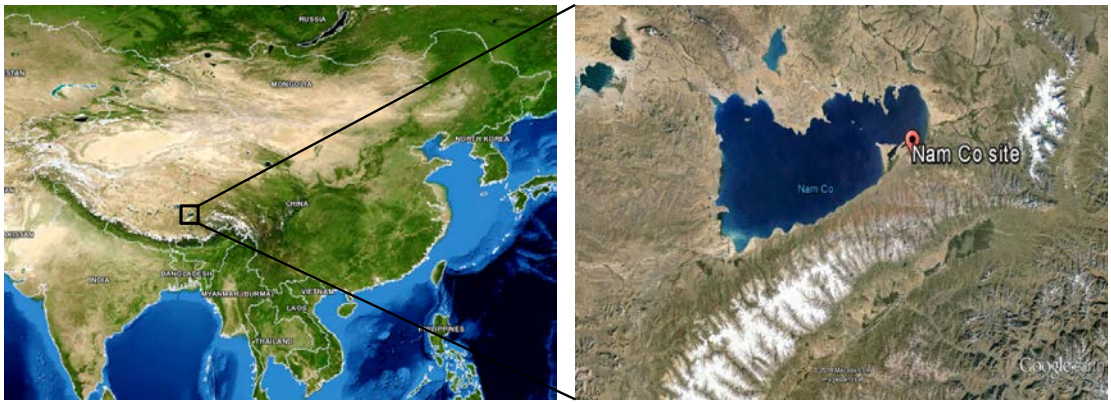

Figure 1 Nam Co site in the Tibetan Plateau, China

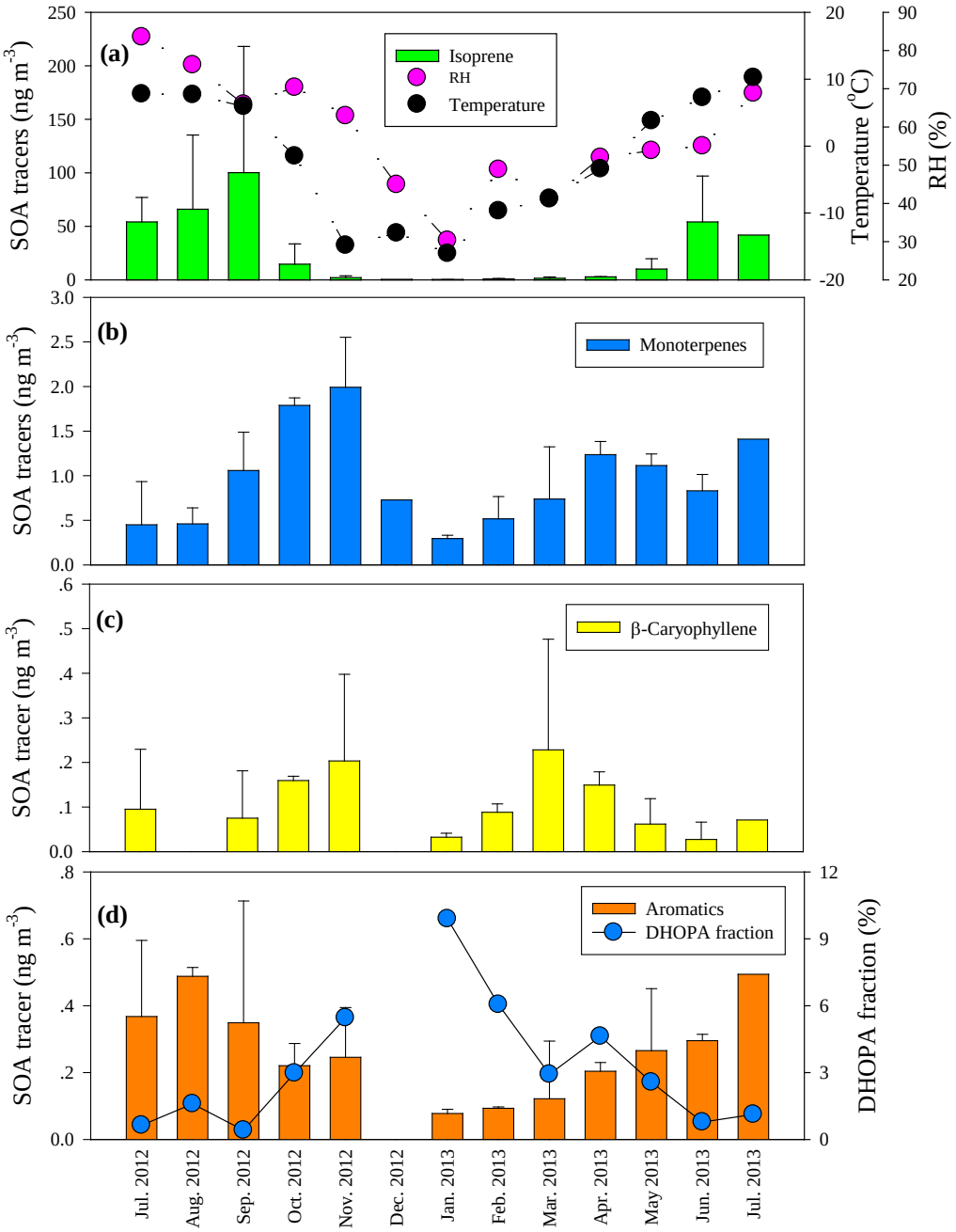

661

662 Figure 2 Monthly variations of SOA tracers.

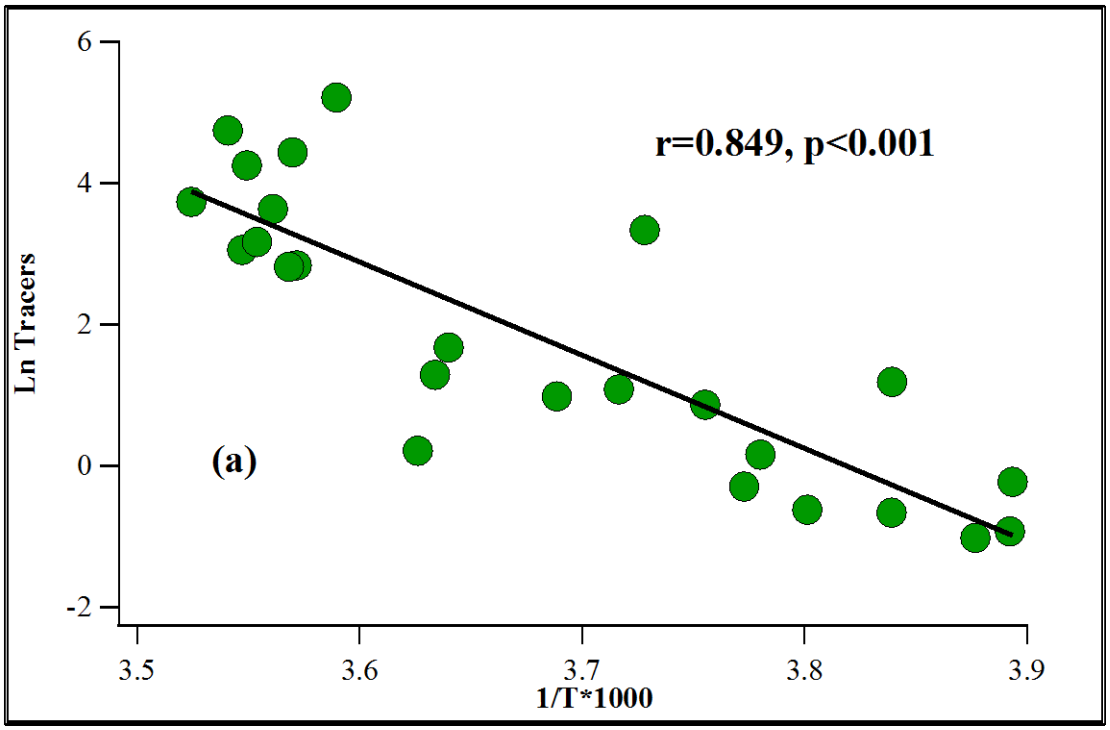

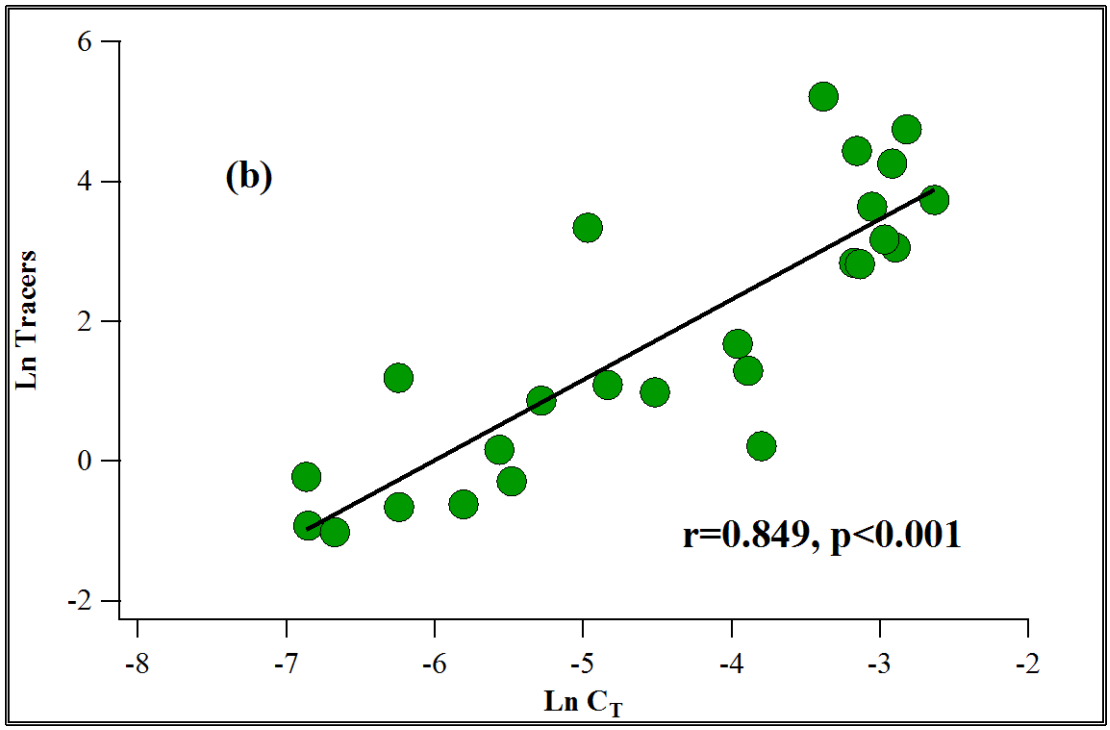

Figure 3 Correlations of SOA_I tracers with temperature (a) and C_T (b).

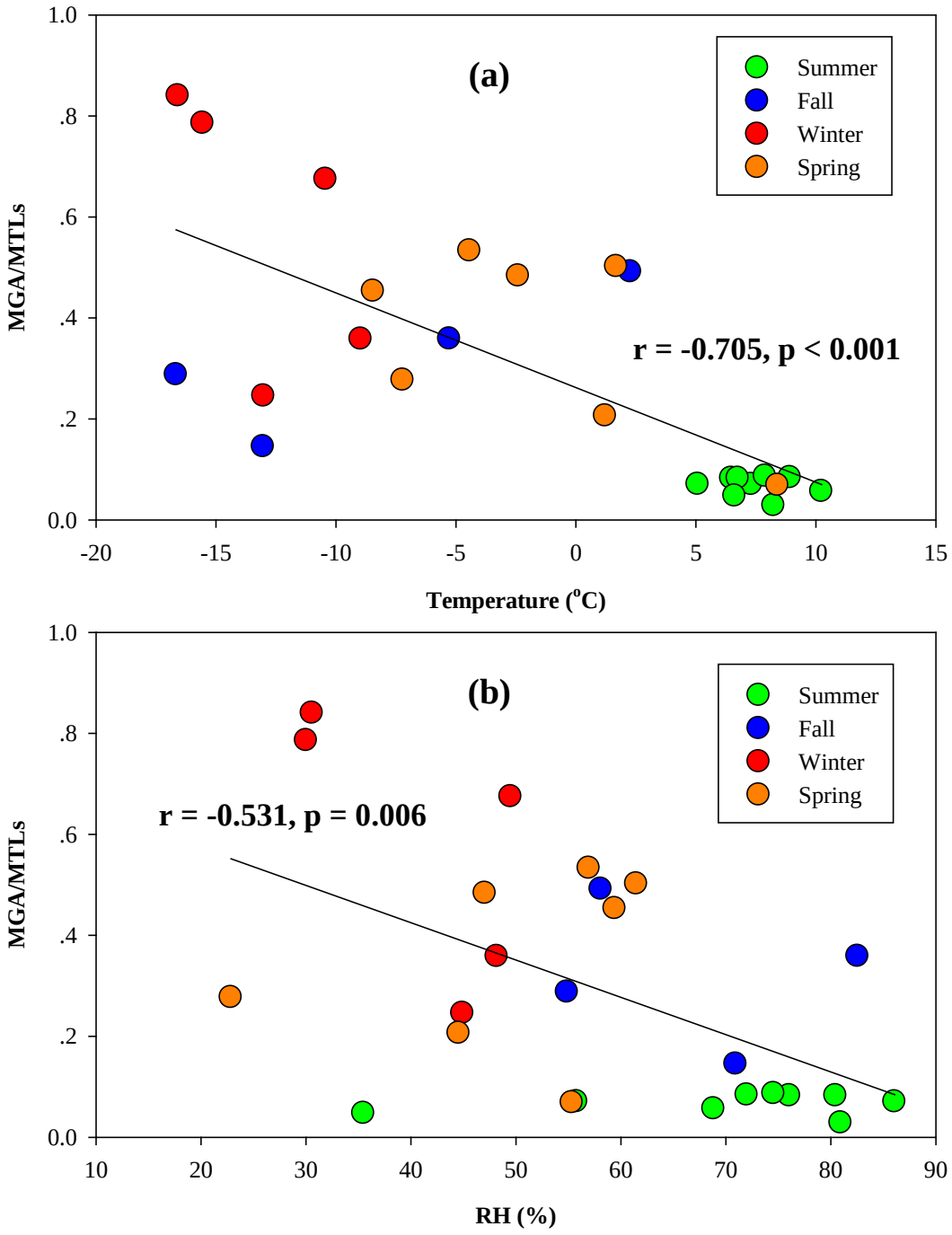

Figure 4 Correlations of MGA/MTL with temperature (a) and relative humidity (b). Summer is from July to September 2012 and from June to July 2013, fall is from October to November 2012, winter is from December 2012 to February 2013, and spring is from March to May 2013.

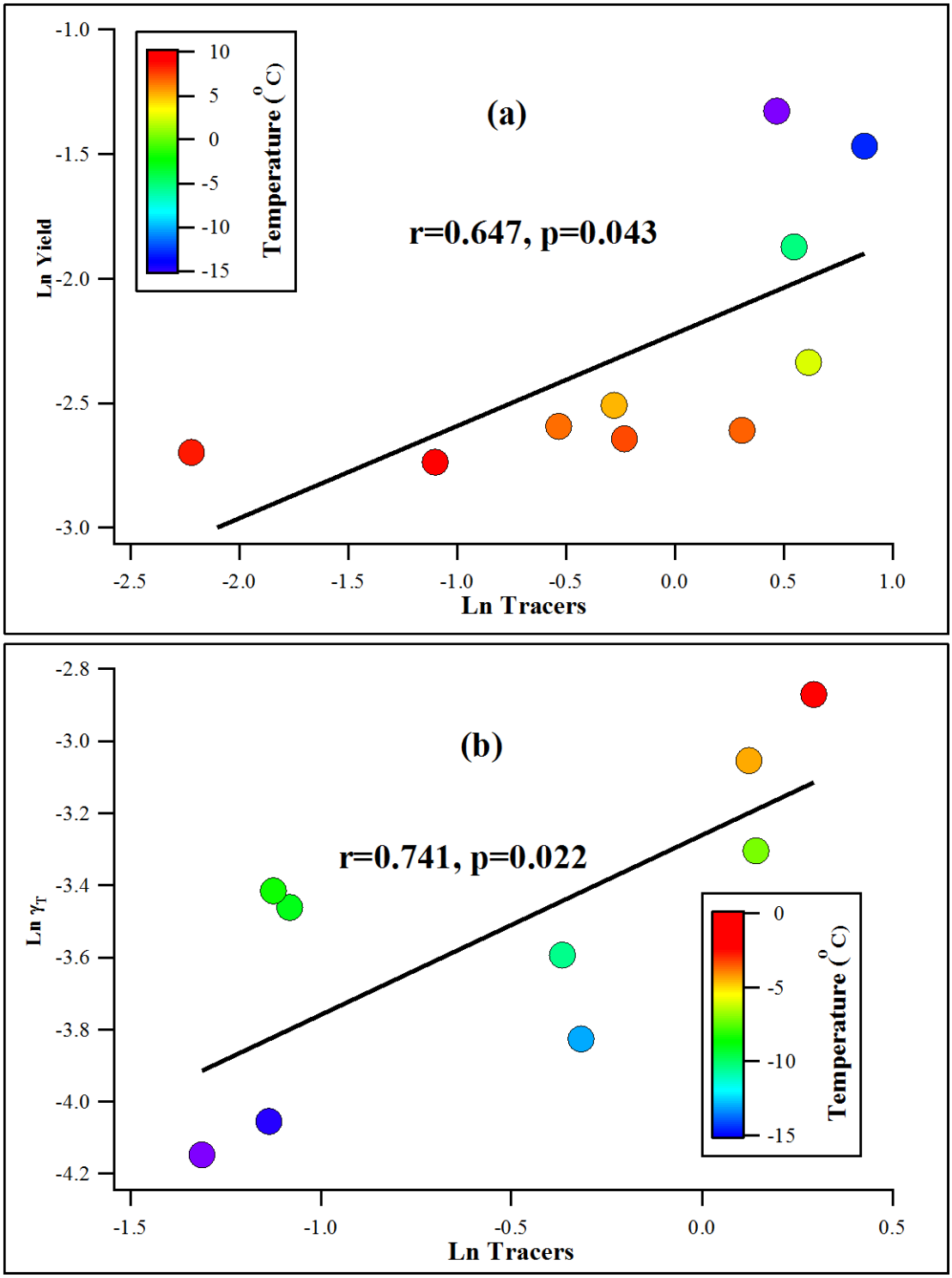

673

674 Figure 5 Correlation of SOA_M tracers with SOA yield in period 1 (a) and γ_T in
675 period 2 (b)

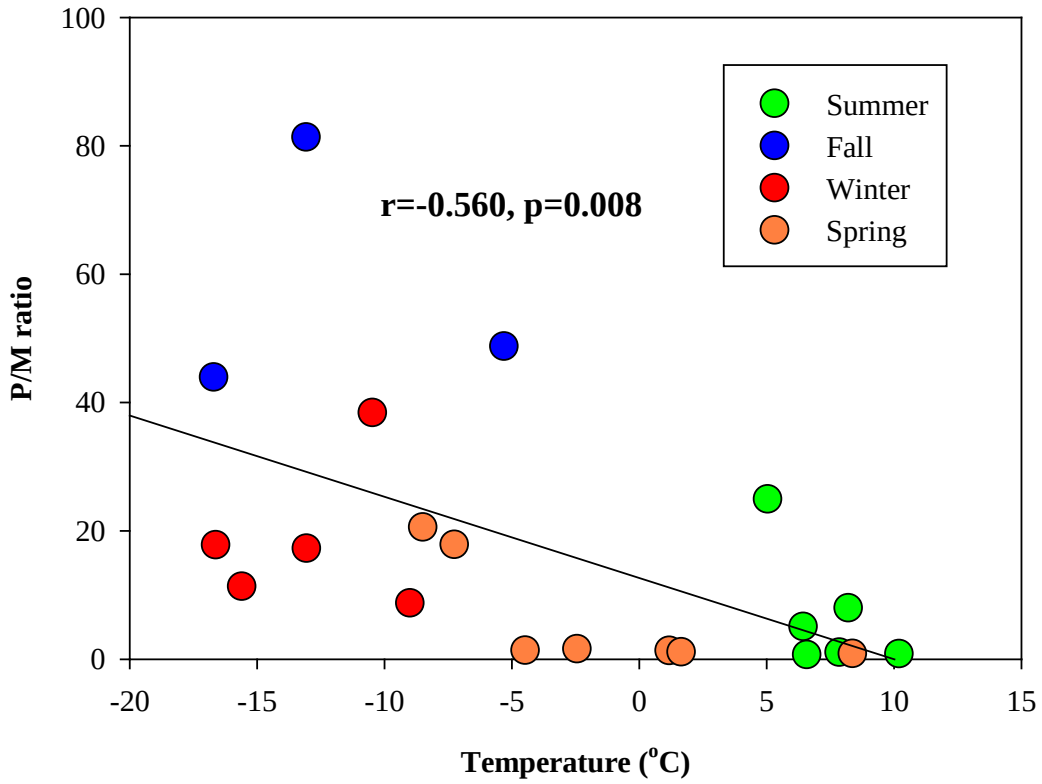

676

677 Figure 6 Negative correlation between P/M ratio and temperature

678

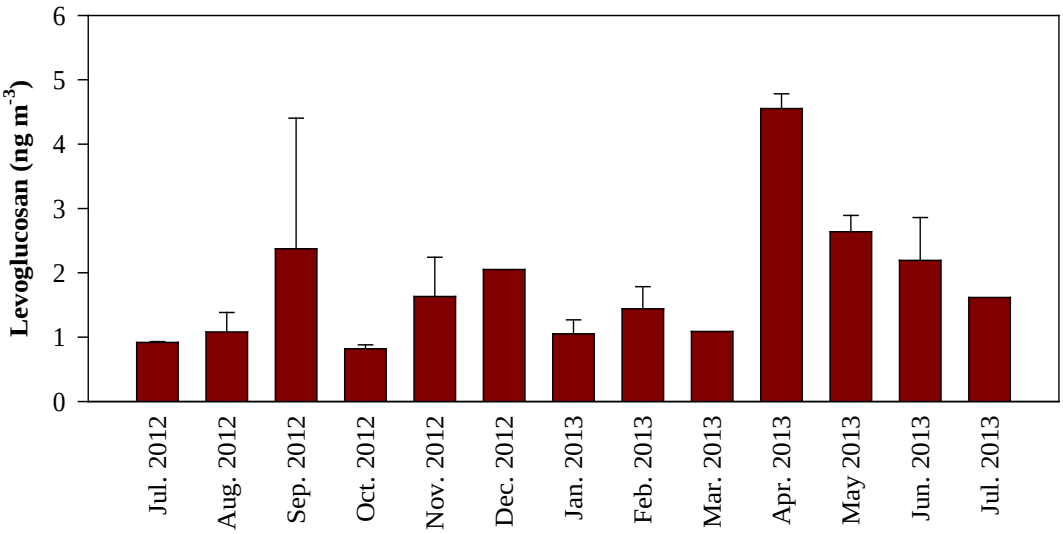

679

680 Figure 7 Monthly variation of biomass burning tracer, levoglucosan

681

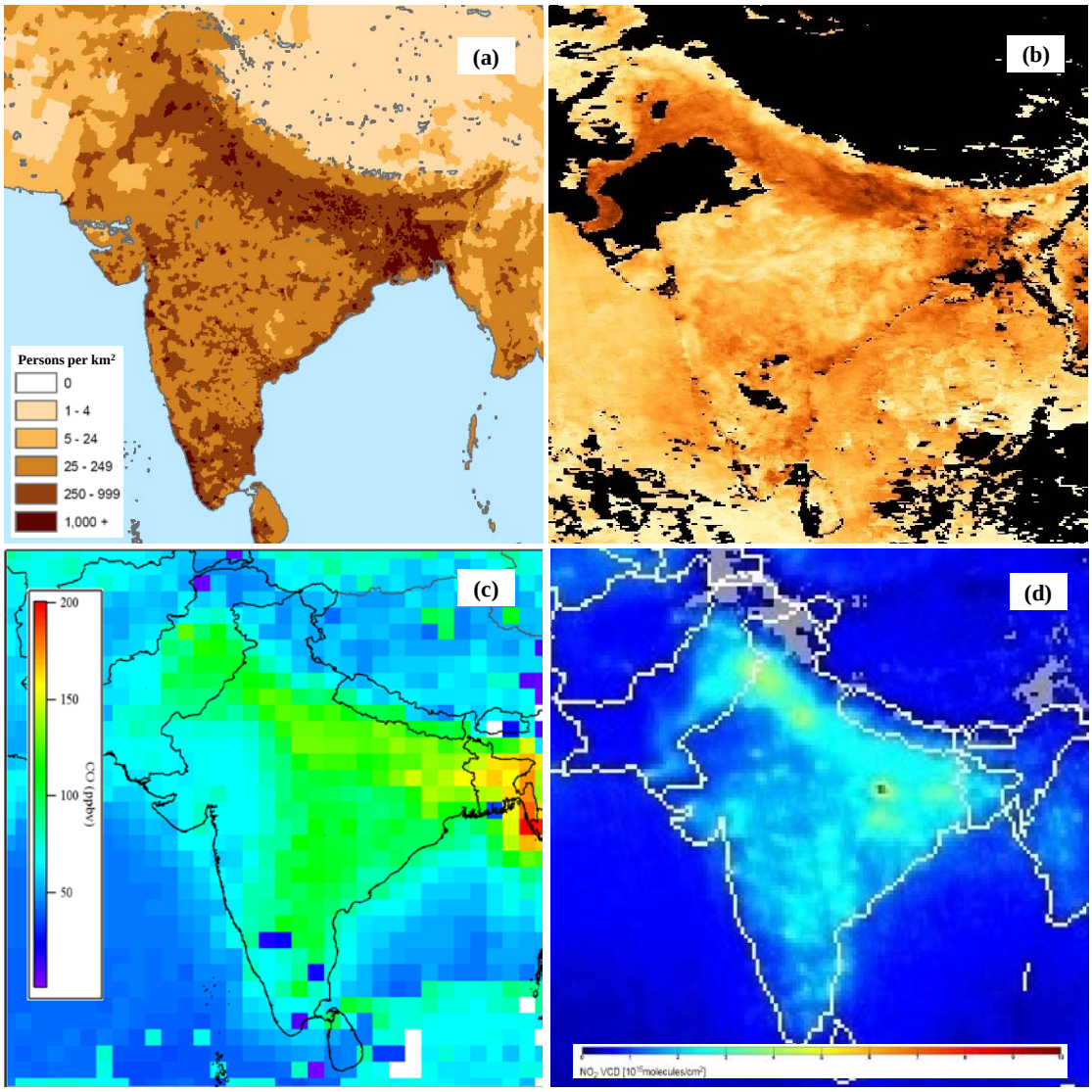

Figure 8 Spatial distribution of population density in 2000 (a), AOT (b), surface CO (c), and NO_2 VCD (d) in May 2013 over the Indian subcontinent and the TP.

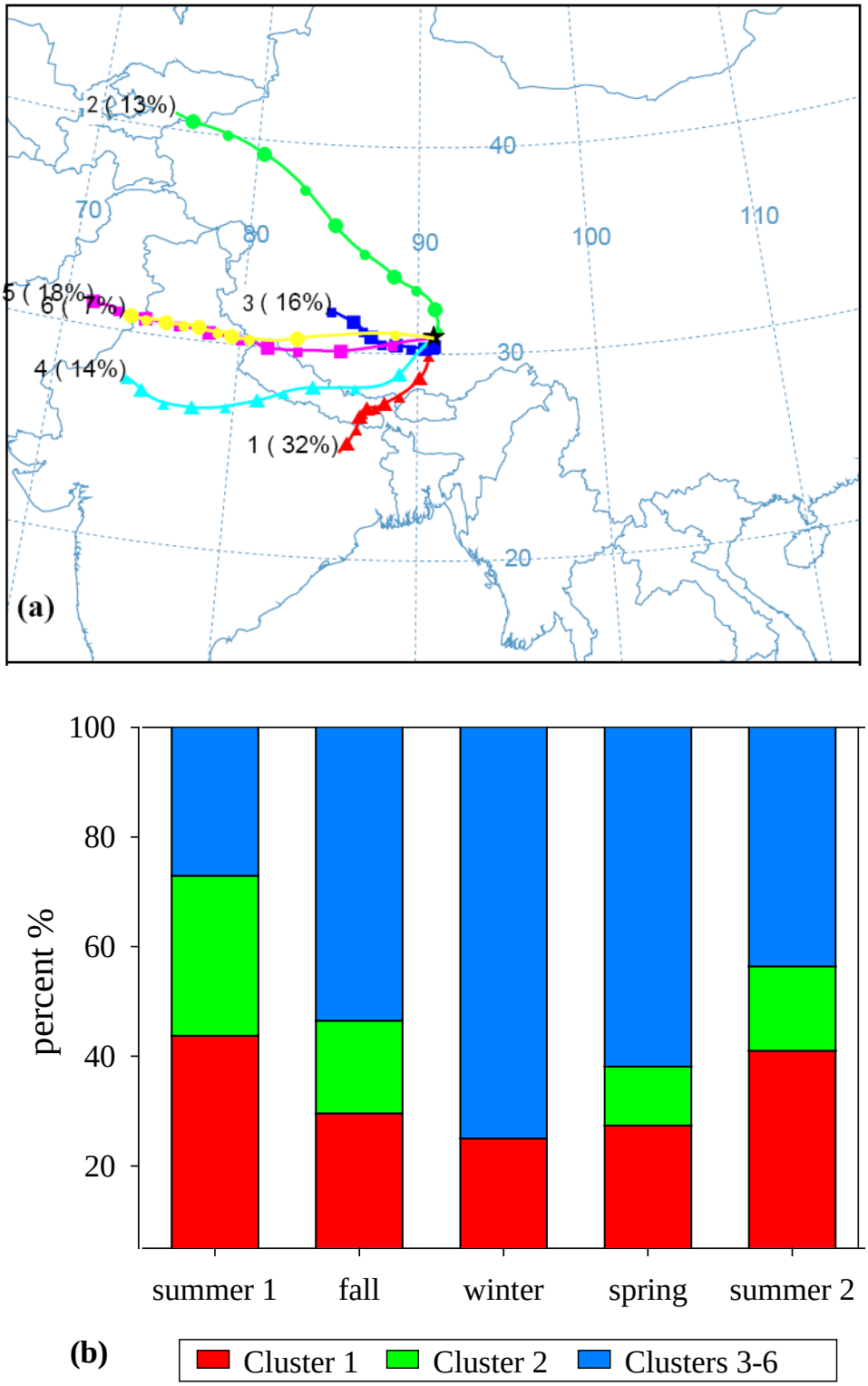

685

686

687 Figure 9 Cluster analyses of air masses at the NC site (a) and seasonal variations of clusters (b), based

688 on 5-day backward trajectories during the sampling period. Summer 1 is from July to September 2012,

689 fall is from October to November 2012, winter is from December 2012 to February 2013, spring is

690 from March to May 2013, summer 2 is from June to July 2013.

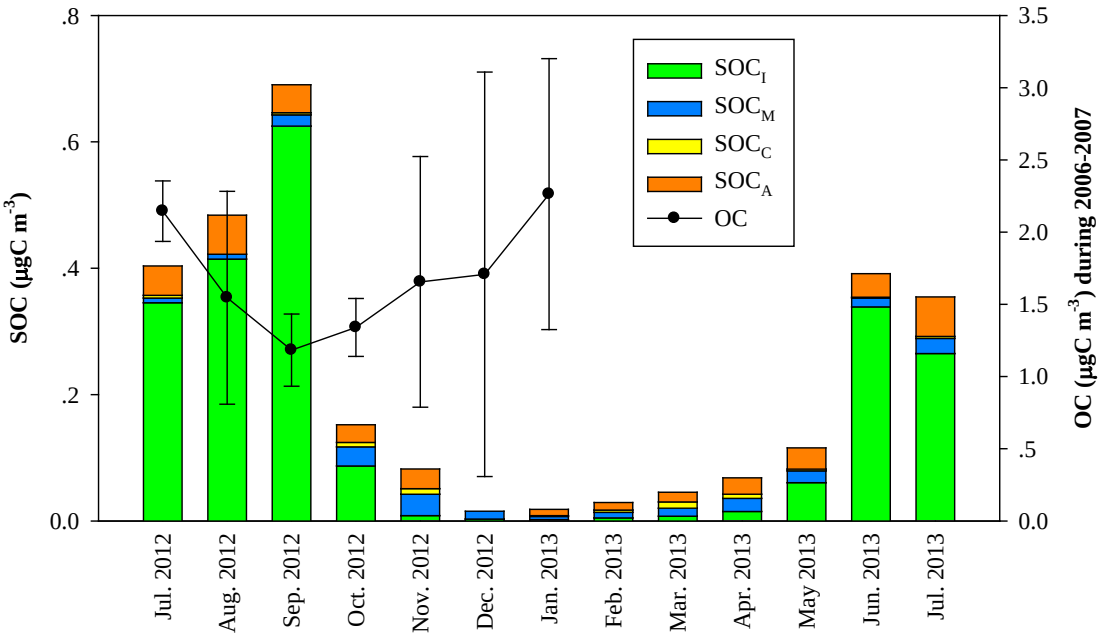

691

692 Figure 10 Seasonal variations of estimated SOC. OC data at the NC site during July 2006 to January

693 2007 were reported by Ming et al., (2010) and the error bar means one standard deviation in each

694 month.

Table 1 SOA tracers at the NC site (ng m^{-3})

Month	Temp. °C [a]	RH % [a]	SOA tracers				
			Isoprene	Monoterpenes	β-Caryophyllene	Aromatics	Sum
Jul. 2012	7.78	84	54.1±22.9 [b]	0.45±0.48	0.10±0.13	0.37±0.23	55.0±22.5
Aug. 2012	7.70	76	66.0±69.3	0.46±0.18	nd [c]	0.49±0.03	67.0±69.1
Sep. 2012	5.92	66	100±118	1.06±0.43	0.08±0.11	0.35±0.36	102±118
Oct. 2012	-1.50	70	14.7±19.0	1.79±0.08	0.16±0.01	0.22±0.07	16.8±18.9
Nov. 2012	-14.9	63	2.04±1.76	1.99±0.56	0.20±0.19	0.25±0.15	4.48±2.66
Dec. 2012	-13.0	45	0.52	0.73	nd	nd	1.25
Jan. 2013	-16.1	30	0.38±0.02	0.30±0.04	0.03±0.01	0.08±0.01	0.78±0.01
Feb. 2013	-9.69	49	0.86±0.45	0.52±0.25	0.09±0.02	0.09±0.01	1.55±0.22
Mar. 2013	-7.83	41	1.56±1.15	0.74±0.59	0.23±0.25	0.12±0.17	2.65±2.15
Apr. 2013	-3.42	52	2.82±0.20	1.24±0.15	0.15±0.03	0.20±0.03	4.40±0.11
May 2013	3.77	54	10.1±9.70	1.11±0.13	0.06±0.06	0.27±0.19	11.5±9.97
Jun. 2013	7.25	55	54.1±42.9	0.83±0.18	0.03±0.04	0.30±0.02	55.3±42.8
Jul. 2013	10.2	69	41.9	1.41	0.07	0.49	43.9
Annual	-1.64	58	26.6±44.2	0.97±0.57	0.09±0.10	0.25±0.18	28.0±44.2

[a] Temperature and RH are monthly averages; [b] one standard deviation; [c] "nd" means not detected.

Table 2 SOA tracers in remote places on the global range (ng m^{-3})

Locations		Seasons	References	SOA tracers			
				Isoprene [a]	**Monoterpenes** [a]	**β-Caryophyllene**	**Aromatics**
Tibetan Plateau	Nam Co Lake	Whole year	This study	26.6(0.36-184) [b]	0.97(0.11-2.39)	0.09(nd-0.40)	0.25(nd-0.61)
	Qianghai Lake	Summer	(Li *et al.* 2013)	2.50(0.13-7.15)	2.95(0.30-10.4)	0.87(0.05-2.41)	na [c]
	Himalayas	Summer-autumn	(Stone *et al.* 2012)	30.7(5.5-105)	13.2(5.6-31.3)	1.6(1.1-2.3)	na
Arctic	Alert	Winter-Summer	(Fu *et al.* 2009)	0.3(0.08-0.567)	1.6(0.138-5.3)	0.12(0.01-0.372)	na
	Arctic Ocean	Summer	(Fu *et al.* 2013)	4.0(0.16-31.8)	4.8(0.44-24.1)	0.017(0.005-0.048)	na
Global oceans	Low- to mid-latitude	Fall-Spring	(Fu *et al.* 2011)	3.6(0.11-22)	2.7(0.02-15)	0.32(0-2.5)	na
	Antarctic to Arctic	Summer	(Hu *et al.* 2013)	8.5(0.018-36)	3.0(0.05-20)	na	na
	North Pacific and Arctic	Summer	(Ding *et al.* 2013)	0.62(0.12-1.45)	0.06(0.01-0.25)	0.002(nd-0.03)	nd [d]

[a] compositions are different in different studies. [b] data range in brackets. [c] "na" means not available. [d] "nd" means not detected.